# Application of Ultraviolet Photoelectron Spectroscopy in the Surface Characterization of Polycrystalline Oxide Catalysts. 2. Depth Variation of the Reduction Degree in the Surface Region of Partially Reduced $V_2O_5$

**M. Heber[†] and W. Grünert***

*Lehrstuhl für Technische Chemie, Ruhr-Universität Bochum, D-44 780 Bochum, Germany*

*Received: November 29, 1999; In Final Form: March 23, 2000*

The surface of partially reduced $V_2O_5$ has been studied by photoemission techniques of different sampling depths (ultraviolet photoelectron spectroscopy (UPS), V (2p) X-ray photoelectron spectroscopy (XPS), and valence-band XPS excited by Mg Kα) in order to investigate the distribution of $V^{4+}$ species in the near-surface region. Reduction was performed by evacuation in ultrahigh vacuum or treatment with flowing hydrogen (10% $H_2$ in Ar) at temperatures between 373 and 923 K. Average reduction degrees were derived from $V^{4+}$ (3d) and O (2p) signals in the valence-band region and from the V ($2p_{3/2}$) signal ($V^{4+}/V^{5+}$ ratio). Comparison of average reduction degrees obtained from different sampling depths showed that pronounced depth profiles of the $V^{4+}$ concentration develop during reduction. At low reduction temperatures, the reduction degree decreases monotonically with the distance from the surface. At higher temperatures, when oxygen mobility in the solid competes with oxygen removal from the surface, the depth profile of the reduction degree changes significantly. During reduction in flowing hydrogen, the maximum of the reduction degree shifts from the outermost surface layer into subsurface layers. A similar effect is likely to occur during reduction by thermal evacuation. The strong inhomogeneities in the near-surface region may lead to significant errors when the reduction state of the outermost surface layer is described on the basis of XPS alone under the assumption of a homogeneous sampling region. This indicates a need for further improvement of the methodology for surface analysis with reduced bulk oxides.

## 1. Introduction

The popularity of X-ray photoelectron spectroscopy (XPS) in heterogeneous catalysis, corrosion, and other fields targeting the particular properties of the gas−solid interface is very much based on the promise that this technique may provide a quantitative analysis of the outermost surface layer of the solid, that is, the atomic layer that terminates the solid and is adjacent to the vacuum or the gas phase. On the other hand, it is well-known that the average sampling depth $\lambda$ of XPS (typically 1.5−2.5 nm depending on the photoelectron kinetic energy) by far exceeds the monolayer dimensions of the materials studied. Hence, XPS integrates over a more or less extended near-surface region, which comprises the outermost layer and subsurface layers. From the general expression for the signal intensity $I_i$ of a species $i$ with the concentration $c_i$ varying with the distance $z$ from the external surface,

$$I_i \propto \sigma_i\, T(E_{kin}) \int_0^\infty c_i(z) \exp(-z/\lambda)\, dz = \sigma_i\, T(E_{kin})\, L\, (c_i(z)) \quad (1)$$

where $\sigma_i$ is the photoionization cross section, $T$ the spectrometer transmission function, $c_i(z)$ the concentration of $i$ varying with $z$, and $L$ the Laplace transformation, it can be deduced that the outermost surface layer usually contributes only 20−30% of the measured signal intensities. Therefore, a direct correspondence between elemental ratios determined by XPS and the composition of the outermost layer exists only if the elemental concentrations are constant throughout the XPS sampling region.

Since such homogeneity of the sampling region is the exception rather than the rule with real materials, there are several techniques allowing the investigation of depth profiles of elemental concentrations without sample destruction by sputtering. These are based on the solution of the Laplace transformation in eq 1 with model assumptions or based on the relative enhancement of outermost surface layer(s) that is achieved when the electrons are collected at directions far from the surface normal (sample-tilting technique; for an informative review covering work with planar model catalysts, see ref 1). Whereas the latter technique gives quantitative information only with planar surfaces because of the compromising effect of particle orientation and grain curvature in polycrystalline materials, the former approach is more general. For systems segregated into a support and a supported phase (e.g., supported metal catalysts), several models are available to evaluate a dispersion parameter (e.g., an average crystal dimension) from information on only one line of the supported element.[2−4] With mixed phases, more than one parameter is required to characterize the distribution of an element (e.g., concentration in the outermost surface layer, width parameter of the depth profile); hence, different lines of an element, with different escape depths, have to be used to provide the relevant depth information. The use of lines with different sampling depths has been shown to be favorable also in the analysis of segregated systems.[5]

While the elemental analysis in the third dimension is well established, it has been rarely considered that similar depth

* To whom correspondence should be addressed. Phone: +49 234 322 2088. Fax: +49 234 3214 115. E-mail: w.gruenert@techem.ruhr-uni-bochum.de.

[†] Present address: Institut für Oberflächen- und Mikrostrukturphysik, Technische Universität Dresden, D-01062 Dresden, Germany.

10.1021/jp994188o CCC: $19.00 
Published on Web 05/16/2000

profiles may exist also for the concentration of ionic species formed during reduction of a high-valence oxide. Such gradients in the reduction degree have to be expected in all cases where the rate of oxygen release into the gas phase is of the same order of magnitude as (or higher than) the rate of oxygen diffusion in the bulk. While this has been known for a long time, there has not been, to our knowledge, an attempt to demonstrate these depth profiles by surface-analytical methods so far presumably because of the limited sampling depth variations provided by the traditional laboratory X-ray sources. For such an attempt, ultraviolet photoelectron spectroscopy (UPS), which is able to probe $d^n$ defects in the bandgap, may provide the required highly surface-sensitive information, most conveniently for $d^1$ defects in the surface of $d^0$ oxides.

In part 1 of this series,[6] which is devoted to practical aspects of UPS with polycrystalline oxides and gives an overview of the opportunities in this field, the existence of depth variations of the $V^{4+}$ concentration in mildly reduced $V_2O_5$ has been demonstrated. The present paper reports a detailed study of such depth profiles in partially reduced $V_2O_5$ on the basis of measurements with photoelectrons of different sampling depths (UPS, below 1 nm; V (2p) XPS, ~1.5 nm; valence-band XPS, above 2 nm). The evaluation of profile shapes is demonstrated, and the consequences of these inhomogeneities for surface-analytical reduction studies with bulk oxides are discussed.

## 2. Experimental Section

**2.1. Materials and Measurements.** $V_2O_5$ was prepared from $NH_4VO_3$ (Janssen Chemica; p.a. grade). All gases employed were provided by Messer-Griesheim and of >99.999% purity. Mixtures were prepared in in-house facilities. $V_2O_5$ was obtained by calcination of $NH_4VO_3$ (4 h in 20 vol % $O_2/N_2$ at 773 K). Its phase purity was identified by X-ray diffraction analysis (XRD), and its BET surface was determined by a one-point BET technique to be 3.5 $m^2/g$. Scanning electron micrographs and XRD reflectance intensity ratios indicated that the material has the typical platelet morphology of $V_2O_5$ with preferential exposition of the (010) plane.[7]

Surface analytical investigations were performed with a Leybold LHS 10 instrument equipped with a EA 10/100 multichannel detector (Specs). The base pressure in the vacuum system was routinely $<10^{-9}$ mbar, with the residual gas formed mainly by species desorbing from the powdered samples. Prior to any measurement, the $V_2O_5$ samples were oxidized for 1 h at 573 K in 20% $O_2/N_2$ (60 mL/min) at normal pressure to remove any surface defects.[6] Reductive treatments were performed either by heating in ultrahigh vacuum in the analysis chamber of the spectrometer (thermoevacuation) or by reduction in flowing hydrogen at normal pressure (10 vol % $H_2$ in Ar, 30 mL/min). The samples were heated to the preselected temperature at typically 1 K/s. After a 1 h isothermal period (±1 K) they were cooled to room temperature at the same rate. Oxidation pretreatment and reduction in hydrogen were done in the fast insertion lock of the spectrometer; hence, samples could be evacuated and transferred into ultrahigh vacuum (UHV) without any contact with the ambient atmosphere. After the hydrogen treatments, the evacuation pressure in the UHV system was typically between $10^{-8}$ and $10^{-9}$ mbar, the residual gas being formed by molecules desorbing from the sample surface. In one case (Figure 7), a prereduction of the sample was performed by etching the surface with Ar ions for 1 h (1000 eV, ion current of 5 $\mu A/cm^2$ at normal incidence). This treatment aimed at the production of surface defects without the intention of establishing a particular reduction degree in the near-surface region.

Photoemission from these samples was studied at room temperature (with some exceptions indicated below)—first, the He(II) ultraviolet photoelectron (UP) spectra, which were recorded with the analyzer at a constant pass energy of 23.7 eV, subsequently, the X-ray photoelectron (XP) spectra. The latter spectra were generated from excitation using Mg Kα radiation (1253.6 eV at 12 kV and 20 mA) and were recorded at pass energies of 35.5 eV (V (2p)/O (1s) region) and 82.9 eV (valence band (VB)). For control purposes, the V (3p) and O (2s) signals (at 42 and 21.6 eV binding energy, respectively) were measured together with the XPS valence band. Since sample charging was absent, the binding energies (BE) were determined relative to the Fermi level. From analyses of the C (1s) region, carbon impurities on the samples were found to be absent or at an extremely low level. No changes of the spectra during data acquisition was noted; that is, there were no indications of reduction of the surface under the influence of the photon sources.

Prior to further data treatment, correction for satellites was performed with the software package "Macfit",[8] which deconvolutes the satellites out of the raw data instead of using a subtraction procedure. In He(II) UPS, the satellite (He(II)$\beta$)/main-line ratio may vary with the He pressure in the discharge lamp. By use of the facility of "Macfit" for user-defined satellite/main-line ratios, the ratios were chosen to reduce any intensity above the Fermi level to zero.

**2.2. Data Treatment.** Figure 1 presents typical spectra obtained by UPS and XPS (V (2p) region) and exemplifies their analysis. Both in UPS and valence-band XPS, the valence band was fitted by three Voigt-type lines on a Shirley background as shown in Figure 1a for the UP spectrum. The choice of the Shirley background was justified by only the moderate incline of the baseline in the binding-energy range between 15 and 10 eV (Figures 2a and 3b). It should be noted that the fit was performed to assess the area of the valence-band signal. No attempt was made to cover particular weak features by individual signals, as seen by a comparison of Figure 1a with the raw spectrum shown in Figure 2a (673 K). The fact that the lines appear to reflect the position and width of the main features is not meant to indicate that these may be interpreted as signals arising from individual states.

Isotropic or average reduction degrees ($\bar{\rho}$) were calculated from the $V^{4+}$ (3d)/O (2p) area ratios using effective photoionization cross sections, which were derived from the subshell cross sections and asymmetry parameters tabulated by Yeh and Lindau[9] with angles between source and detector, $\gamma$, of 135 ° in UPS and 120 ° in XPS (see Table 1). The subshell cross sections in these tables refer to the atomic electron configuration ($3d^3$ and $2p^4$ for V and O, respectively).[9] For the evaluation of cross sections of valence-band electrons in a partially covalent system, it is in principle necessary to calculate these cross sections from the wave functions. Since this was not possible, an estimate was made on the basis of recent ab initio DFT calculations of the $V_2O_5$ electron structure by Hermann et al.[10] Their results, obtained by both a cluster approach and a periodical approach, imply that vanadium contributes 20−25% to the density of states in the valence band, where the lower limit is provided by the periodical calculations. Table 1 reports estimates of the ionization cross sections based on an ionic approach (O 2 $p^6$/V $3d^0$) and a covalent approach where the vanadium contribution has been taken to be 25% (O $2p^{4.5}$/V $3d^{1.5}$). From these data, it is obvious that the influence of covalency should be negligible with UV excitation. In the X-ray-excited valence-band spectra, the cross-section is significantly

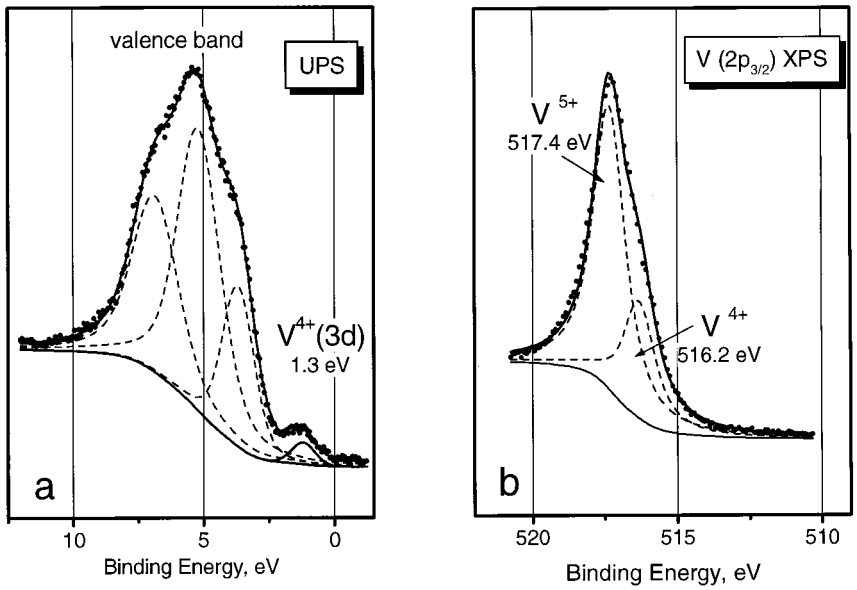


**Figure 1.** Analysis of valence-band and V ($2p_{3/2}$) XP spectra: (a) valence band, He(II) excitation, where the valence-band shape has been formally represented by three lines; (b) V($2p_{3/2}$) line. For constraints employed in the signal shape analysis see text.

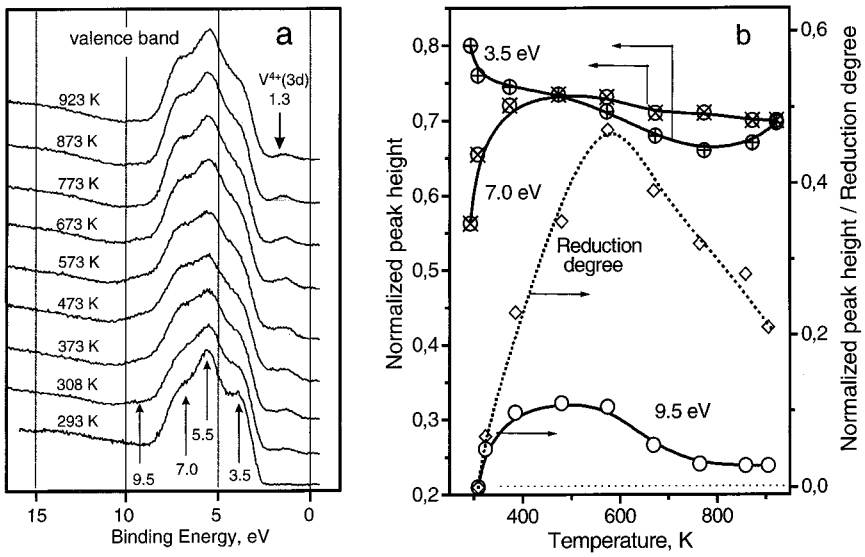


**Figure 2.** UPS of $V_2O_5$ reduced by treatment in ultrahigh vacuum at elevated temperatures: (a) UP spectra, $V^{4+}$ contribution shaded (by hand); (b) development of spectral features with the reduction temperature and comparison with the average reduction degree. Heights of features at 3.5, 7.0, and 9.5 eV are normalized to the height of the central feature (5.5 eV). The average reduction degree has been taken from Figure 4.

**TABLE 1: Effective Cross Sections for the Evaluation of Reduction Degrees from Signal Areas in UPS and XPS (Derived on the Basis of Ref 9), in barns**

| | (for given electron configuration) | |
|---|---|---|
| | $\sigma$ (1253.6 eV) | $\sigma$ (40.8 eV) |
| O ($1s^2$) | $70.88 \times 10^3$ | |
| O ($2s^2$) | $3.263 \times 10^3$ | |
| O ($2p^6$) | 777.3 | $8.550 \times 10^6$ |
| valence band, "ionic"[a] | 130 | $1.43 \times 10^6$ |
| valence band, "covalent"[a] | 171.6 | $1.53_5 \times 10^6$ |
| V ($2p^4_{3/2}$) | $153.9 \times 10^3$ | |
| V ($3p^6$) | $22.89 \times 10^3$ | |
| V ($3d^1$) | $297.9_5$ | $1.867 \times 10^6$ |

[a] Per electron.

affected by the character of the electrons, with the "covalent" estimate probably indicating an upper limit.

The V ($2p_{3/2}$) XPS signal was fitted by two Voigt-type lines of equal line shape ($V^{5+}$, $V^{4+}$), the Gaussian/Lorentzian contributions of which were fixed to the values obtained from the spectrum of unreduced $V_2O_5$ (Figure 3a, 295 K, experimental line width 1.3 eV). This yielded binding energies of 517.4 and 516. 2 eV for $V^{5+}$ and $V^{4+}$, respectively. Both values are well in the range of binding energies given for these states in the literature.[11−15] The reduction degrees obtained from the $V^{4+}$/$V^{5+}$ ratios were confirmed by similar calculations of the basis of the $V^{4+}$ ($2p_{3/2}$)/O (1s) intensity ratios.

The choice of line widths in the analysis of superimposed V (2p) signals is a matter of controversy. In studies with bulk oxides, it was found that $VO_2$ and $V_2O_3$ exhibit much broader V (2p) lines than $V_2O_5$ (typical ranges reported:[16] 1.3−1.5 eV for $V_2O_5$, ca. 2.5 eV for $VO_2$ (nonmetallic state, at room temperature, 3.4 eV in the metallic state at $T > 341$ K [15]), 4.5−4.8 eV for $V_2O_3$). A trend to higher line widths of reduced species may arise from multiplet splitting, and different line widths for $V^{n+}$ ($n = 3, 4, 5$) have been indeed employed in the analysis of spectra taken from $VO_x/ZrO_2$ catalysts.[17] On the other hand, reduction studies with $V_2O_5$[13] and $V_2O_5/TiO_2$ catalysts[14] at low reduction degree provided V (2p) signal shapes that were

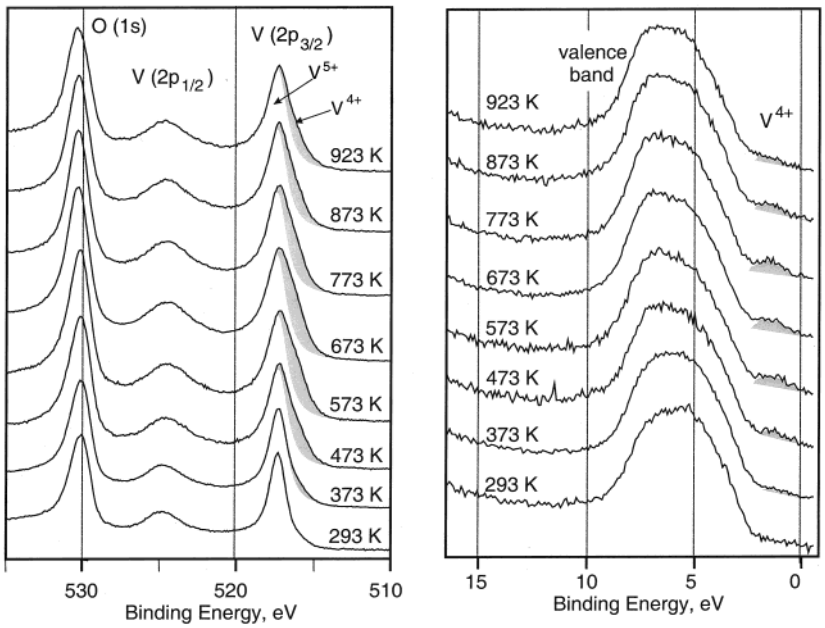


**Figure 3.** XPS of $V_2O_5$ reduced by treatment in ultrahigh vacuum at elevated temperatures: (a) V (2p)/O (1s) region, $V^{4+}$ contribution shaded (from calculations); (b) valence-band region, $V^{4+}$ contribution shaded (by hand).

definitely incompatible with line widths of about 2−3 eV and yielded almost identical fwhm for $V^{5+}$ and $V^{4+}$. The same is true with our spectra, where the reduction degree was large enough in many samples to give the $V^{4+}$ state sufficient weight to determine the shape of the low-energy side of the superimposed signal. It proved impossible to fit a $V^{4+}$ signal of 2.5 eV fwhm to our spectra as would be expected for $VO_2$. We could, indeed, exclude the formation of the $VO_2$ structure even at the highest reduction degrees by measuring UP spectra at 473 K where intensity at the Fermi level due to metallic $VO_2$ was never observed. When the condition of identical line width was dropped in the analysis of V (2p) signals, the $V^{4+}$ fwhm increased by 10% at maximum, the $V^{4+}$ ($2p_{3/2}$) binding energy changed by 0.1−0.2 eV, and the reduction degree determined was affected by not more than 5% (rel). Hence, in nonordered structures, the $V^{4+}$ line width is obviously close to that of the $V^{5+}$ signal, as assumed in our V (2p) signal shape analysis.

In spectra containing contributions of the $V^{3+}$ state, the corresponding line was found at 514.9 eV, which is at the lower limit of the range reported in the literature (515.0−515.7 eV [16,18,19]). For $V^{3+}$, some increase of the line width due to multiplet splitting is quite likely. Preliminary analyses with released constraint on the $V^{3+}$ (2p) line width showed, however, that possible errors due to the simplified analysis are too small to affect the conclusions derived below.

For control purposes, average reduction degrees were also derived by evaluation of V/O elemental ratios—via the V (3p)/O (2s) signals for the sampling depth covered by the valence-band spectra and via the V ($2p_{3/2}$)/O (1s) signals for the V (2p)/O (1s) sampling depth. Although the reliability of the intensity data appears to be good (with the ionization cross sections employed, the $V_2O_5$ surface stoichiometry as measured via V ($2p_{3/2}$) and O (1s) amounted to $V_2O_{4.9}$), the accuracy of these data is limited because the $V^{5+} \rightarrow V^{4+}$ reduction studied in our project removes only a small part of the oxygen. Hence, these data were used only to prove the absence of major inadequacies in the final results.

The reduction degrees $\bar{\rho}$ measured at different sampling depths (UPS, V (2p), VB-XPS) are the average over a region in which $\rho$ may vary with the depth coordinate $z$. The local solid composition may be written as $V^{5+}_{(1-\rho)}V^{4+}_{\rho}O_{(2.5-0.5\rho)}$. When $c(V^{4+},z) = c_{0,V}\rho(z)$, $c(V^{5+},z) = c_{0,V}(1 - \rho(z))$, and $c(O,z) = c_{0,O}(2.5 - \rho(z))$ (with $c_{0,V}(c_{0,O})$ being the vanadium (oxygen) atom concentration), the average reduction degrees are, for the example of the V (2p)/O (1s) region,

$$I(V^{4+}(2p)) \propto \sigma_{V(2p)}\, T(E_{kin})\, c_{0,V}\, L\,(\rho(z)) \qquad (2a)$$

$$I(V^{5+}(2p)) \propto \sigma_{V(2p)}\, T(E_{kin})\, c_{0,V}(\lambda - L\,(\rho(z))) \qquad (2b)$$

and

$$I(O(1s)) \propto \sigma_{O(1s)}\, T(E_{kin})\, c_{0,O}(2.5\lambda - 0.5L\,(\rho(z))) \qquad (2c)$$

When the profiles $\rho(z)$ are represented by particular mathematical functions, a numerical analysis of these depth profiles becomes possible by fitting the parameters of these functions to reproduce the measured reduction degrees for different sampling depths. For this analysis, the mean free electron path $\lambda$ has to be known while the spectrometer transmission function $T$ cancels because the reduction degrees are derived from lines with similar kinetic energy. In the present study, a correlation proposed by Seah and Dench for oxide materials[20,21] has been employed to estimate $\lambda$ (in nm) at different photoelectron kinetic energies $E_{kin}$ (in eV). The equations used also provide an estimate for the thickness of a monolayer $a_M$ (in nm)

$$\lambda = a_M\left(\frac{2170}{E_{kin}^{\ 2}} + 0.55\sqrt{a_M E_{kin}}\right) \qquad (3)$$

with

$$a_M = 10^8\sqrt[3]{\frac{A_M}{\rho_M N_A}} \qquad (4)$$

($A_M$ is the mean atomic weight in g mol$^{-1}$, $\rho_M$ is the density in kg m$^{-3}$ of the material studied, $N_A$ is Avogadro's constant). The resulting values are given below in section 4.

## 3. Results

Figure 2a shows a series of UP spectra recorded after reducing $V_2O_5$ by thermal evacuation in UHV for 1 h at the specified

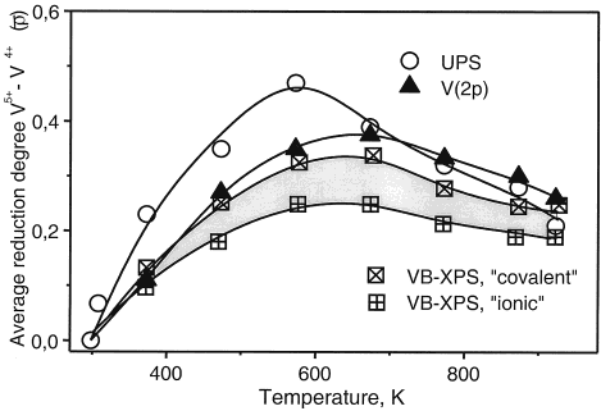


**Figure 4.** Surface analysis of partially reduced $V_2O_5$ (reduction by thermoevacuation) by signals arising from different sampling depths. Average reduction degrees are from UPS ($\lambda = 0.78$ nm), V (2p) XPS ($\lambda = 1.67_5$ nm), and valence-band XPS ($\lambda = 2.21$ nm). Reduction degrees derived from the XPS valence band are expected to be in the range indicated by the shaded area. The range is defined by data evaluated with the "ionic" and "covalent" estimates (Table 1) of the photoionization cross-section (lower and upper limits, respectively).

temperatures. This treatment causes distinct changes in both the range of the valence band between 3 and >9 eV and in the bandgap. The (oxidized) initial sample, measured at 295 K, exhibits a well-defined valence-band shape with a maximum at 5.5 eV and pronounced shoulders at 3.5 and 7.5 eV. With increasing temperature, a $V^{4+}$ (3d) signal appears at ~1.3 eV but decreases again above 573 K. At the same time, the shoulder at 3.5 eV decreases with increasing temperature, but at the highest temperatures it becomes more pronounced again. The opposite tendency may be noted with the 7.5 eV shoulder, which first becomes more intense with increasing temperature but decays at the upper end of the temperature range. Additionally, a new shoulder emerges around 9.5 eV, which is quite pronounced between 373 and 573 K but significantly weaker at high temperatures. These tendencies have been summarized in Figure 2b where the heights of the features normalized to the height of the 5.5 eV maximum have been plotted versus the evacuation temperature and compared with the average reduction degrees derived from the V (3d)/O (2p) intensity ratio (Figure 4). It can be seen that the shoulders at 7.0 and 9.5 eV exhibit a similar tendency as the reduction degree while the 3.5 eV shoulder behaves opposite. However, this correlation is merely qualitative, and there is disagreement between the temperatures at which the minimum of the 3.5 eV shoulder and the maxima the remaining features occur.

Figure 3 reports XP spectra acquired from the same samples. It is quite clear that the V ($2p_{3/2}$) line (Figure 3a) becomes broader with increasing temperature up to 573 K. Above 673 K, the line width decreases again. The O (1s) line is slightly asymmetric and suffers a small shift to higher binding energies (~0.3 eV), but no significant change in the signal shape can be noted over the whole series. In the XPS valence-band spectra (Figure 3b), both the O (2p) and the $V^{4+}$(3d) signals are less resolved than in the UV-excited spectra (Figure 2a). Nevertheless, it is quite clear that $V^{4+}$ has an analogous tendency to increase with a subsequent decrease also in the XPS valence-band region.

In Figure 4, the average reduction degrees $\bar{\rho}$ deduced from the spectra shown above under the assumption of a homogeneous sampling region are plotted versus the evacuation temperature. Up to 600 K, $\bar{\rho}$ is clearly larger in the UPS sampling region than in the regions with higher sampling depth, but above this temperature, the UPS-derived reduction degree decays most steeply. The relation between the V (2p) and the VB-XPS sampling regions depends on the cross-section estimate applied for the latter (section 2.2 and Table 1). The "ionic" estimate provides reduction degrees clearly lower than in the V (2p) region, while little difference remains when the "covalent" estimate is applied. This leads to quite different descriptions of the near-surface region. With the "covalent" estimate, all three average reduction degrees may be considered identical at $T \geq 673$ K; i.e., a homogeneous sampling region is established under these conditions. It should be noted, however, that a decrease of the reduction degree with increasing reduction temperature results from this assumption. With the "ionic" estimate, the homogeneous sampling region is established only at 923 K, while the UPS-derived reduction degree is still significantly larger than that found in the XPS valence-band region up to 873 K.

Figure 5 presents spectra recorded after reduction of the $V_2O_5$ sample in flowing hydrogen (10 vol % $H_2$ in Ar) at different temperatures. Up to 773 K, signals of reduced states are weak in all three sampling regions. However, comparison of the UP spectra (Figure 5a) with that of the initial (reoxidized) $V_2O_5$ (Figure 2a, 293 K) proves that there *is* significant intensity at 1.3 eV, which remains at approximately the same level up to 773 K. At 873 and 973 K, the V(3d) signal is clearly more intense. The trends of the valence-band features at 3.5, 7.0, and 9.5 eV are similar as observed during thermoevacuation. It should be noted that the intensity of the 9.5 eV shoulder never becomes more intense than in the thermoevacuation series.

In the XP spectra (Figure 5b,c), the reduction of the $V_2O_5$ surface below 773 K is even more difficult to detect while above 873 K the changes are much more pronounced than in the UPS region. This is immediately clear upon comparing the UP and valence-band XP spectra (Figure 5a,c). The V ($2p_{3/2}$) lines measured after reduction at $T \geq 873$ K had to be represented by three vanadium lines ($V^{5+}$, $V^{4+}$, $V^{3+}$) as indicated in the Experimental Section (section 2.2.).

Figure 6 reports the development of the average reduction degrees $\bar{\rho}$ evaluated from the spectra shown in Figure 5. To remain in the formal framework of a $V^{5+} \rightarrow V^{4+}$ reduction, the amount of $V^{3+}$ detected was replaced by twice the amount of $V^{5+}$ reduced to $V^{4+}$. At low temperatures, the average reduction degrees obtained by UPS are higher than those obtained in the remaining sampling regions. Thorough comparison with the reference spectra in Figure 3 (295 K) shows that some reduction is indicated by the XP spectra as well, but it is clear that at low reduction degrees a large error may occur in particular in the analysis of the V (3d) state in VB-XPS, so the data given in Figure 6 for this sampling region are, certainly, too high. At $T \geq 873$ K, there is strong divergence in the extent of reduction in the sampling regions compared. The UPS-derived reduction degree is lowest, while at 873 K there is a pronounced maximum of the reduction degree in the V (2p) sampling region.

## 4. Discussion

The data presented above confirm the expectation that the near-surface region of a partially reduced oxide may be inhomogeneous owing to the competition between oxygen removal by the reductant and oxygen migration in the oxide crystal. Both during reduction of $V_2O_5$ by thermal evacuation and in flowing hydrogen, the reduction degrees measured for the smallest sampling depth (UPS) exceed those obtained for more extended sampling regions at low temperatures; i.e., the outermost surface layer is the most reduced (Figures 4 and 6). The situation changes between 573 and 673 K for thermal

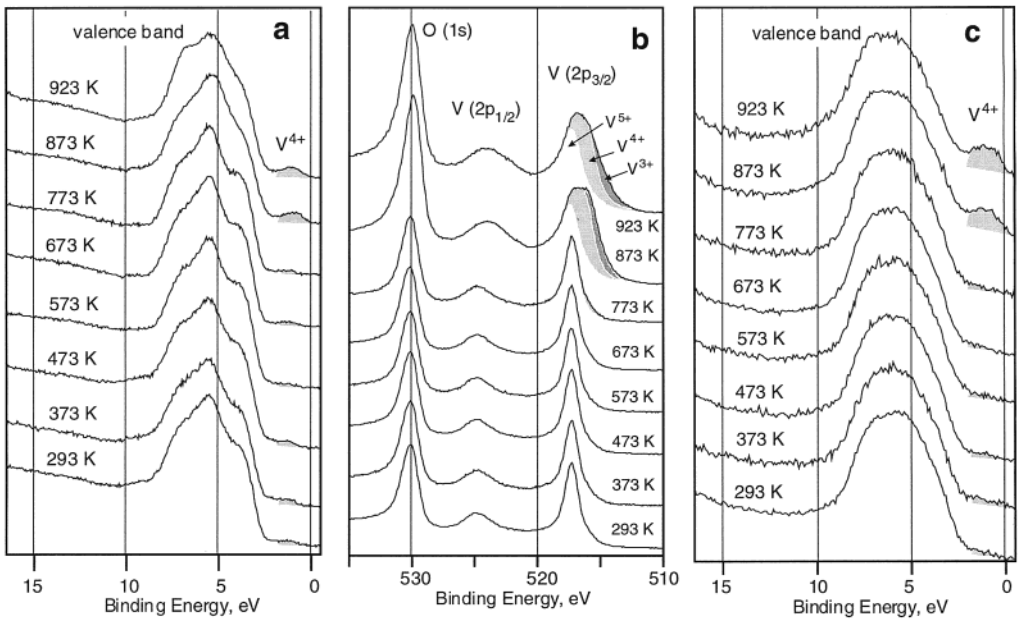


**Figure 5.** UPS and XPS of $V_2O_5$ reduced in flowing hydrogen (10% $H_2$/Ar): (a) UP spectra, $V^{n+}$ contribution ($n = 4$ for $T \leq 773$ K) shaded (by hand); (b) XPS, V (2p)/O (1s) region, $V^{4+}$ and $V^{3+}$ contributions shaded (from calculations); (c) XPS, valence-band region, $V^{n+}$ contribution ($n = 4$ for $T \leq 773$ K) shaded (by hand).

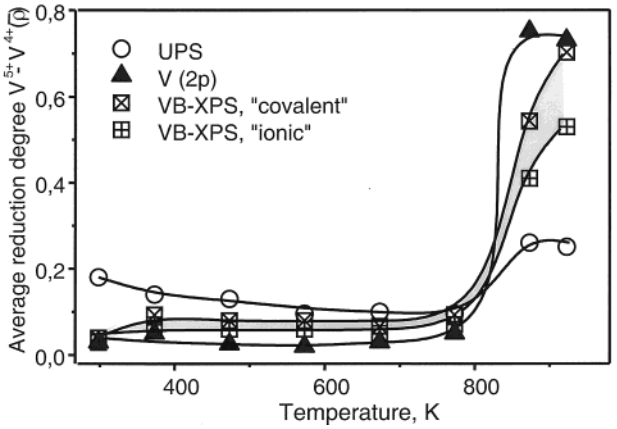


**Figure 6.** Surface analysis of partially reduced $V_2O_5$ (reduction in a flowing $H_2$/Ar mixture, 10 vol % $H_2$) by signals arising from different sampling depths. Average reduction degrees are from UPS ($\lambda = 0.78$ nm), V (2p) XPS ($\lambda = 1.67_5$ nm), and valence-band XPS ($\lambda = 2.21$ nm). Reduction degrees derived from the XPS valence band are expected to be in the range indicated by the shaded area. The range is defined by data evaluated with the "ionic" and "covalent" estimates (Table 1) of the photoionization cross-section (lower and upper limits, respectively).

evacuation and between 773 and 873 K for reduction in hydrogen. In the latter case, there is clear evidence that the maximum reduction degree may occur in subsurface layers. At 873 K, the highest reduction degree is found in the intermediate sampling region (V (2p)) while the less or more depth-integrating techniques (UPS or VB-XPS) see the sample less reduced. Further details depend on the choice of the photoionization cross section in the VB-XPS region.

In the thermoevacuation experiment, the reduction degrees determined from the XPS valence band under the assumption of the "covalent" cross-section estimate (Table 1) cannot be distinguished in the limits of experimental error from the values obtained from the V (2p) region (Figure 4). This implies that at each temperature we have a certain, nearly invariant $V^{4+}$ concentration in the deeper layers predominantly probed by V (2p) and VB-XPS. At low temperatures only, there is excess $V^{4+}$ in the outermost surface layers(s), which is reflected in the UPS signal, while at higher temperatures no measurable gradients occur in the whole near-surface region probed in these measurements.

This picture is unrealistic for several reasons. First, above 673 K, the reduction degree decreases with increasing temperature. This is highly unlikely in an experiment under an oxygen partial pressure well below $10^{-11}$ mbar, which was estimated on the basis of residual-gas analyses performed in our spectrometer. The decrease cannot be accounted for by transient effects, since no gradients of the reduction degree that could drive a flux of oxygen anions toward the surface can be identified. Moreover, at low temperatures the $V^{4+}$ excess concentration in the outermost layer(s) is obviously due to the low oxygen mobility under these conditions. It is then not easy to explain why the deeper layers have already attained a finite reduction degree that remains almost constant along the $z$ coordinate. To determine under which conditions oxygen mobility becomes detectable in our samples, we performed an analogous thermoevacuation experiment with a $V_2O_5$ sample previously sputtered with Ar ions (section 2.1). In the UP spectra shown in Figure 7a, the surface reduction of the initial sample (293 K) is indicated by an intense defect signal at 1.5 eV and the lack of structure in the valence-band region. Up to 573 K, there is little change in the spectral shape, but at $T \geq 673$ K, the defect signal decreases significantly. The surface $V^{n+}$ ($n = 3, 4$) becomes reoxidized obviously by oxygen migration and at the expense of bulk $V^{5+}$. Thus, at $T \leq 573$ K the oxygen mobility appears to be insufficient to allow the formation of extended reduced subsurface regions during thermoevacuation.

The description of the near-surface region under the assumption of the "ionic" cross-section estimate for the XPS valence band is quite different. Now, the reduction degree obtained from VB-XPS is the lowest for all temperatures less than or equal to 923 K (Figure 4). For the low-temperature region, this shows that we have indeed a continuous decay of the $V^{4+}$ concentration in deeper layers. For $T \geq 673$ K, the data imply that the maximum of the reduction degree has shifted into subsurface layers. Indeed, UPS and V (2p) XPS provide equal average

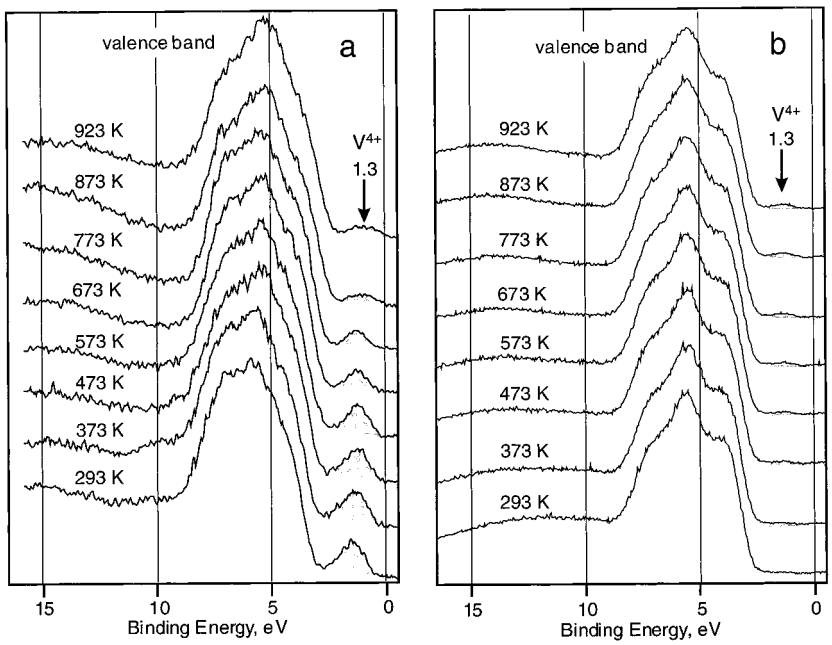


**Figure 7.** Influence of the oxygen mobility and of the oxygen partial pressure on the thermoevacuation of $V_2O_5$: (a) UP spectra obtained after treating a Ar-etched $V_2O_5$ surface (initial spectrum labeled "293 K") in ultrahigh vacuum at elevated temperatures; (b) UP spectra measured under a background oxygen pressure of $2 \times 10^{-7}$ mbar (oxygen dosed onto the sample) at elevated temperatures.

reduction degrees $\bar{\rho}$ while that probed by VB-XPS remains significantly lower. Since the probing depths of V (2p) and VB-XPS overlap to a large extent, the $\bar{\rho}$ value measured by V (2p) must contain contributions from regions with lower reduction degree (at larger $z$). As a consequence, there must be regions with $\rho > \bar{\rho}$ (V (2p)) at lower $z$. These are, however, not adjacent to the vacuum results because $\bar{\rho}$ (UPS) does not exceed $\bar{\rho}$ (V (2p)). Hence, the maximum of $\rho(z)$ is below the outermost surface layer.

This can be demonstrated by a numerical analysis of the depth profiles of the $V^{4+}$ concentration, which has been performed on the basis of eqs 2a−2c as outlined in the Experimental Section (section 2.2.) using average reduction degrees obtained with the "ionic" cross-section approach for VB-XPS. Mean free electron paths were used as obtained from eqs 3 and 4 with $\rho_M = 3.357 \times 10^{-3}$ kg m$^{-3}$ and $A_M = 25.8$ g mol$^{-1}$: 0.78 nm for UPS ($E_{kin} = 35$ eV), $1.67_5$ nm for the V (2p)/O (1s) region ($E_{kin} = 720$ eV), and 2.21 nm for the XPS valence-band region ($E_{kin} = 1260$ eV). The monolayer thickness according to eq 4 was 0.234 nm. The profiles were assumed to be Gaussian (centered at the external surface, eq 5) or a Gauss profile multiplied by a first-order polynomial (eq 6)

$$\rho(z) = \rho_0 \exp\left(-\frac{z^2}{2\Delta^2}\right) \tag{5}$$

$$\rho(z) = \rho_0 \sqrt{e}\,\frac{z}{\Delta} \exp\left(-\frac{z^2}{2\Delta^2}\right) \tag{6}$$

The parameters $\rho_0$ and $\Delta$ were varied by an exhaustive search algorithm to find the mimimum of the mean square deviation between calculated and measured average reduction degrees (see ref 36).

Figure 8 presents the depth profiles of the reduction degree derived on this basis. The numerical values of the profile parameters $\rho_0$ and $\Delta$ are given in the figure. For 373 K, these values are $\rho_0 = 1.16$ and $\Delta = 1.49$ Å; i.e., $\rho_0$ is beyond the physical limit $\rho = 1$. We conclude from this that the defects

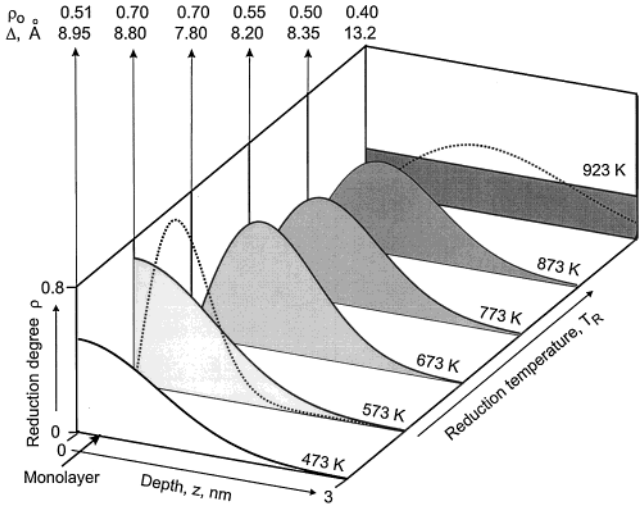


**Figure 8.** Variation of the reduction degree with the distance from the external surface upon 1 h evacuation of $V_2O_5$ in ultrahigh vacuum at elevated temperatures. Analysis was performed on the basis of average reduction degrees using the "ionic" cross-section estimate for VB-XPS. For a mathematical form of the profiles see eqs 5 and 6. Parameters obtained by fitting these equations to the experimental average reduction degrees (Figure 4) are given in the figure. The monolayer extension is indicated by an arrow.

are confined to the outermost surface layer at this temperature. At 473 and 573 K, the depth profiles of the $V^{4+}$ concentration are well represented by a Gauss distribution, which fails, however, above 573 K. At 573 K the experimental data were equally well fitted by eqs 5 and 6, but reduction degrees in excess of 1 were provided by the latter (Figure 8, dotted curve at 573 K). Since there was no indication in XPS that $V^{3+}$ may have been formed by thermoevacuation, this solution was rejected.

At higher temperatures, the Gaussian distribution is clearly inadequate and the profiles are well represented by eq 6. The maximum of the reduction degree goes into the subsurface region. With increasing temperature, the profiles become broader and the maximum shifts deeper into the solid. Up to 873 K,

however, the profiles do not become flat. At 923 K only, the evaluated curved profile may be considered inadequate because the small differences between the average reduction degrees measured with different kinetic photoelectron energies indicate that the model of the isotropic sampling region has now been approached. The latter conclusion is also supported by the comparison between the average reduction degrees calculated from the profiles and those derived from the V(total)/O intensity data (V (2p)/O (1s) and V (3p)/O (2s)). Below 923 K, these agree within $\pm 10\%_{rel}$ for the V (2p)/O (1s) region and within $\pm 20\%_{rel}$ for the valence-band region. At 923 K, however, the deviations were $23\%_{rel}$ and $60\%_{rel}$, respectively; i.e., the average reduction degree was inadequately reproduced by the curved profile.

While the shift of the most reduced area into subsurface layers at higher temperatures is unexpected at first sight, it should be noted that the overall description of the reduction process contains no inconsistencies as obtained by the use of the "covalent" cross-section estimate. It appears, therefore, that the "ionic" cross-section estimate is more realistic, and the real situation is likely to be reflected by Figure 8 at least on a qualitative basis. A more quantitative description would require the use of vanadium core levels at different sampling depths, which is the subject of current research in our group. The shift of the most reduced region into the solid, which is in effect a dissolution of $V^{4+}$ defects in the subsurface layers, may be caused by a gain in entropy. A similar case of surface reoxidation under reducing conditions has been recently observed with Ce/Zr/O mixed oxides by Daturi et al.[22] in an infrared spectroscopic analysis of surface Ce valence states via frequency shifts of OH vibrations.

The description of the near-surface region after reduction in hydrogen (Figure 6) is less affected by the choice of the cross-section estimate for the XPS valence band. At low temperature, the VB-XPS data are subject to large numerical error anyway, as mentioned above. The relation between $\bar{\rho}$ from UPS and V (2p) XPS indicates that the $V^{4+}$ defects are confined to the outermost (one or two) surface layer(s) under these conditions. At $T \geq 873$ K, the outermost layer is less reduced than the subsurface layers. There is a maximum of the reduction degree below the surface at 873 K, and probably still at 923 K, as indicated by the data evaluated with the "ionic" cross-section estimate.

These results may be related to the literature about the temperature-programmed reduction (TPR) of $V_2O_5$, for example.[23,24] It is known that during TPR no hydrogen consumption can be observed below 773 K while the reduction peaks appear at considerably higher temperatures ($\geq$873 K). Our measurements are in good agreement with these reports, but additionally, our results show clearly that $V^{4+}$ is present in the outermost surface layer at temperatures far below the onset of measurable hydrogen consumption. The reduced species can be a result of reduction by hydrogen, but they also can have been formed by thermal desorption of oxygen as in the thermoevacuation experiment. The extent to which these processes contribute to the observed surface reduction is not known.

The low reduction degree of the outermost surface layer compared with the situation produced by thermal evacuation at the same temperatures (Figures 6 and 4) is surprising at first sight. We believe that this is due to different oxygen partial pressures in the two experiments: $p_{O2}$ is well below $10^{-11}$ mbar in the UHV experiment as mentioned above while $10^{-6}$ mbar ($10^{-3}$ ppm) $O_2$ is already of brilliant purity in terms of a flow experiment at normal pressure.

To confirm this idea, we performed a thermoevacuation experiment analogous to that documented in Figures 2 and 3 but with an oxygen background pressure of $2 \times 10^{-7}$ mbar. The oxygen was dosed through a quartz capillary directly onto the sample, and the effective oxygen partial pressure felt by it was estimated to be $10^{-6}-10^{-5}$ mbar on the basis of kinetic gas theory. Figure 7b summarizes the UP spectra measured, while the sample was held at the specified temperatures. A comparison with Figure 2 shows that the reduction is strongly attenuated by an oxygen partial pressure on the order of $10^{-6}$ mbar, although it is not completely suppressed.

From this it appears likely that the level of the surface $V^{4+}$-concentration, which is established in a hydrogen flow at temperatures below the onset of deep reduction, will depend strongly on the gas purity, as should have been expected. Moreover, the pronounced depth profiles occurring at higher temperatures (Figure 6; $\bar{\rho}$ (UPS) and $\bar{\rho}$ (VB-XPS) $< \bar{\rho}$ (V (2p))) are possibly also influenced by the residual oxygen content of the reducing gas. While it still has to be investigated how sensitive the reduction degree of the outermost layer responds to an oxygen content of ppm and sub-ppm level under such strongly reducing conditions, it may be anticipated that in many systems, the oxygen partial pressure will be a major parameter that influences the steepness of the depth profiles near the surface and the properties of the outermost layer in partially reduced oxides. This implies also that in a (bulk) oxide catalyst utilized in a feed mixture of a given redox potential, the oxidation state of the catalytically relevant outermost surface layer may differ from that of the subsurface layer. This difference should depend on the development of the redox potential along the catalyst bed and experience complicated transient changes in response to changes in the process parameters.

It is quite clear from the results discussed so far that the assumption of a homogeneous sampling region is rather the exception than the rule in the analysis of partially reduced oxide surfaces. It appears that in our experiments, this assumption was fulfilled only after thermal evacuation at 923 K. The depth variations of the reduction degree cast an unfavorable light on the significance of reduction studies with massive oxides performed by XPS alone. With our samples, XPS underestimated the reduction degree of the outermost surface layer at low temperatures, while a serious overestimation occurred at high temperatures in the hydrogen reduction experiment. An analogous trend was most likely present in the thermoevacuation experiment because only the "ionic" cross-section estimate for VB-XPS, which is the basis of the analysis shown in Figure 8, provided a consistent interpretation of all experimental data. Even though the profile shapes assumed are strongly simplified (realistic profiles should not be continuous but stepwise; the condition $\rho(z=0) = 0$ imposed by eq 6 may be too rigid), it is obvious that the situation in the outermost layer changes from $V^{4+}$ enrichment to depletion upon temperature increase so that XPS would first underestimate, then overestimate the surface reduction degree without giving notice under which conditions the situation changes, i.e. when the analysis is correct.

It appears therefore that XPS analyses of partially reduced oxide surfaces may easily lead to incorrect conclusions about the properties of the outermost surface layer. This problem should be less serious with supported oxides, which usually form very thin, often monatomic layers on the support. These layers will not be able to accommodate strong inhomogeneities and are, in addition, often completely within the XPS sampling depth. With bulk oxides, however, depth profiles of the reduction

degree are very likely in all cases where the reduction has not led completely to a very stable final product (e.g., the metal) and in cases after contact of the surface with a reaction mixture of intermediate redox potential as in selective oxidation reactions. Further studies of depth variations of ionic concentrations in partially reduced oxides and development of methodics in this field (e.g., to include $d^{n+}$ ($n > 1$) states) are needed to improve the tools for surface characterization with such materials. It may be anticipated that a future methodology for surface analysis of bulk catalysts will include the use of XPS with synchrotron radiation.

Finally, the changes in the $V_2O_5$ valence-band shape as summarized in Figures 2a and 5a will be briefly discussed. Since the band-structure calculations of Hermann et al.[10] offer the chance to differentiate vanadyl oxygen (V=**O**) and bridging oxygen (V−**O**−V) by their contributions to the valence-band signal, it may be expected that these changes reveal which type of oxygen is removed upon reduction. The question of whether vanadia (unsupported or on titania carriers) participates in oxidation catalysis via the vanadyl or the bridging oxygen is a matter of controversy. The earlier view that these catalysts provide vanadyl oxygen for nucleophilic attack on hydrocarbon reductants (reviewed, for example, in refs 25 and 26) is questioned by a series of recent studies of support influences on catalytic activity of V in various reactions[27−30] showing the deciding role of the oxygen bridging between V and the support cation. In surface science, STM[31] and X-ray photoelectron diffraction[32] studies imply that vanadyl oxygen is removed upon reduction of $V_2O_5$ (010) or imperfect cleavage of crystals along this plane. On the other hand, theoretical studies by Witko et al.[33,34] indicate that bridging oxygen is more reactive than vanadyl oxygen, and UP spectra measured with $V_2O_5$ crystals cleaved in (010) orientation have been interpreted to support this view.[10]

According to ref 10, the valence-band feature at 5.5 eV (Figure 2a) is almost exclusively due to vanadyl oxygen while the shoulder at 7.0 eV is dominated by contributions of bridging oxygen. The 3.5 eV feature arises from bridging and vanadyl oxygen at a ratio of ∼2:1. The shoulder appearing at 9.5 eV upon reduction is not far from the position at which emissions from OH groups are expected ($3\sigma$ state, >10 eV [35]). However, this feature is present already after thermoevacuation in UHV (Figure 2a) and is not significantly increased when the reduction is performed in 0.1 bar hydrogen (Figure 5a). Moreover, there is no evidence for the formation of new OH groups upon thermoevacuation or hydrogen reduction in XPS (Figures 3a and 5b). Therefore, we attribute the feature at ∼9.5 eV to band bending in the vicinity of the $V^{4+}$ defects; i.e., a certain percentage of the valence-band signal is shifted by ∼1.3 eV to higher binding energies.

This band-bending feature complicates the discussion of the valence-band shape to an extent that prevents any definite conclusions at the present time. The split of the valence-band intensity into a majority part at the previous position and a shifted minority part should lead to a relative decrease of the 3.5 eV feature and an increase of the 7.0 eV shoulder, which is indeed observed. To what extent the observed changes are covered by this effect and which modifications of the valence-band shape will remain after the correction for the band-bending shift are not easy to decide. Since any reliable conclusion concerning this point will require an in-depth analysis of the experimental valence-band shapes together with quantum chemical calculations of $V_2O_5$ surfaces with $V^{4+}$ defects, we have left this problem for future research.

## 5. Conclusions

Partially reduced $V_2O_5$ has been studied by photoemission techniques of different sampling depths (UPS, V (2p) XPS, valence-band XPS) to probe variations of the reduction degree with the distance from the external surface. Average reduction degrees $V^{5+} \rightarrow V^{4+}$ derived from spectra measured after thermoevacuation or reduction in flowing hydrogen (10% $H_2$ in Ar) at various temperatures imply the presence of pronounced depth profiles of the $V^{4+}$ concentration. At low temperatures, the $V^{4+}$ concentration decays monotonically with the distance from the surface. At higher temperatures, the character of the depth profiles changes significantly. During reduction in hydrogen the maximum of the reduction degree was found to shift into subsurface layers. A similar trend is implied by the results obtained from $V_2O_5$ heated in ultrahigh vacuum. In almost all samples studied, the condition of a homogeneous sampling region, on which XPS analyses of oxide surfaces are often based, was violated. The results suggest that significant inhomogeneities in the XPS sampling region are rather the rule than the exception with partially reduced oxides and that there is a need for further refinement in the analysis of depth variations of the reduction degree in order to improve the methodology for surface analysis with these types of material.

**Acknowledgment.** We gratefully acknowledge financial support by the Deutsche Forschungsgemeinschaft.

## References and Notes

(1) Gunter, P. L. J.; Niemantsverdriet, J. W.; Ribeiro, F. H.; Somorjai, G. A. *Catal. Rev.—Sci. Eng.* **1997**, *39*, 77.
(2) Kerkhof, F. P. J. M.; Moulijn, J. A. *J. Phys. Chem.* **1979**, *83*, 1612.
(3) Kaliaguine, S.; Adnot, A.; Lemay, G.; Rodrigo, L. **1989**, *118*, 275.
(4) Léon, V. *Surf. Sci.* **1995**, *339*, L931.
(5) Mark Davis, S. *J. Catal.* **1989**, *117*, 432.
(6) Heber, M.; Grünert, W. *Top. Catal.*, in press.
(7) Schoen, M. Diploma Thesis, Ruhr-Universität, Bochum, Germany, 1997.
(8) Boyen, H.-G. *Macfit, Surface Analysis Software Package*; Institute of Physics, University of Basle: Basle, Switzerland, 1996.
(9) Yeh, J. J.; Lindau, I. *At. Data Nucl. Data* **1985**, *32*, 2.
(10) Hermann, K.; Witko, M.; Druzinic, R.; Chakrabarti, A.; Tepper, B.; Elsner, M.; Gorschlüter, A.; Kuhlenbeck, H.; Freund, H.-J. *J. Electron Spectrosc. Relat. Phenom.* **1999**, *98−99*, 245.
(11) Wagner, C. D. In *Practical Surface Analysis*, 2 ed.; Briggs, D., Seah, M. P., Eds.; Wiley: Chichester, 1990; Vol. 1, Appendix 5.
(12) Zhang, Z.; Henrich, V. E. *Surf. Sci.* **1994**, *324*, 133.
(13) Poelman, H.; Fiemans, L. *Solid State Commun.* **1994**, *92*, 669.
(14) Chiarello, G.; Robba, D.; De Michele, G.; Parmigiani, F. *Appl. Surf. Sci.* **1993**, *64*, 91.
(15) Christmann, T.; Felde, B.; Niessner, W.; Schalch, D.; Scharmann, A. *Thin Solid Films* **1996**, *287*, 134.
(16) Mendialdua, J.; Casanova, R.; Barbaux, Y. *J. Electron Spectrosc. Relat. Phenom.* **1995**, *71*, 249.
(17) Ochiuzzi, M.; Tuti, S.; Cordischi, D.; Dragone, R.; Indovina, V. *J. Chem. Soc., Faraday Trans.* **1996**, *92*, 4337.
(18) Sawatzky, G. A.; Post, D. *Phys. Rev. B* **1979**, *20*, 1546.
(19) Smith, K. E.; Henrich, V. E. *Surf. Sci.* **1990**, *225*, 47.
(20) Seah, M. P.; Dench, W. A. *Surf. Interface Anal.* **1979**, *1*, 2.
(21) Seah, M. P. *Surf. Interface Anal.* **1986**, *9*, 85.
(22) Daturi, M.; Finocchio, E.; Binet, C.; Lavalley, J. C.; Fally, F.; Perrichon, V. *J. Phys. Chem. B* **1999**, *103*, 4884.
(23) Bosch, H.; Kip, B. J.; van Ommen, J. G.; Gellings, P. J. *J. Chem. Soc., Faraday Trans. 1* **1984**, *80*, 2479.
(24) Iwamoto, M.; Takenaka, T.; Matsukami, K.; Hirata, J.; Kagawa, S.; Izumi, J. *Appl. Catal.* **1985**, *16*, 153.
(25) Bond, G. C.; Tahir, S. F. *Appl. Catal.* **1991**, *71*, 1.
(26) Bielanski, A.; Haber, J. *Oxygen in Catalysis*; Dekker: New York, 1991.
(27) Wachs, I. E.; Deo, G.; Weckhuysen, B. M.; Andreini, A.; Vuurman, M. A.; de Boer, M.; Amiridis, M. D. *J. Catal.* **1996**, *161*, 211.
(28) Wachs, I. E.; Weckhuysen, B. M. *Appl. Catal. A* **1997**, *157*, 67.

(29) Dunn, J. P.; Stenger, H. G., Jr.; Wachs, I. E. *Catal. Today* **1999**, *51*, 301.
(30) Guliants, V. V. *Catal. Today* **1999**, *51*, 255.
(31) Groschke, R. A.; Vey, K.; Mayer, M.; Walter, U.; Goering, E.; Klemm, M.; Horn, S. *Surf. Sci.* **1996**, *348*, 505.
(32) Devriendt, K.; Poelman, H.; Fiermans, L.; Creten, G.; Froment, G. F. *Surf. Sci.* **1996**, *352*−*354*, 750.
(33) Witko, M.; Tokarz, R.; Haber, J. *Appl. Catal. A* **1997**, *157*, 23.
(34) Witko, M.; Hermann, K.; Tokarz, R. *Catal. Today* **1999**, *50*, 553.
(35) Connor, J. A.; Considine, M.; Hiller, H.; Briggs, D. *J. Electron Spectrosc. Relat. Phenom.* **1977**, *12*, 143.
(36) From eq 5, it follows that at $z = 0$, the reduction degree is $\rho_0$, but this is not the case with eq 6 where $\rho(z=0) = 0$. It should be noted, however, that the reduction degree at $z = 0$ is merely a mathematical quantity. The reduction degree of the first monolayer can be obtained by averaging the $\rho(z)$ profile over the monolayer thickness.